STUDY ON APPLICABILITY OF ALOS DATA FOR FLOOD INUNDATION SIMULATION

PI No. 397

Kazuhiko Fukami[1], Shigenobu Tanaka[1], Hironori Inomata[1] and Hideo Yamashita[1]

International Centre for Water Hazard and Risk Management under the auspices of UNESCO (ICHARM),
Public Works Research Institute, Japan

1. INTRODUCTION

In recent years, flood disasters have been frequent mainly in developing countries, and the situation calls for immediate implementation of flood countermeasures. For this purpose, it is necessary to grasp flood inundation hazardous areas and its-induced damages by simulating possible inundation cases. Numerous researches have been conducted on the matter up until now. However, in most cases, the focus is on basins in developed countries where accurate topography data such as Laser Profiler data (hereinafter LP) is available[1)2)], while few have been done on flood inundation simulation in developing countries where such data is hardly available.

Recently satellite-based topography data with a very fine resolution have become available and expected to be useful for inundation simulation in developing countries. Iwata et al[3)] appears to be the first research in which they applied satellite-based topography data to inundation simulation in Apia, the capital of Samoa, and obtained successful results. Unfortunately, no specific description is provided on the satellite-based topography data they used, and the research findings have had little applicability to other cases.

Considering this background, the main target of this research is to examine the applicability of satellite-based topography data to inundation simulation. More specifically, three types of satellite-based topography data (ALOS PRISM, ASTER and SRTM) available in Japan were used to reproduce an actual flood inundation over the Kariyata River basin in Japan in July 2004. They were also compared in accuracy with LP. In addition, a simple statistical technique was applied to correct the bias of the ALOS PRISM data, and the corrected topography data were applied to reproduce the same inundation case to examine its applicability.

In the next section, the comparison between LP and the other three satellite-based topography data is described. The third section explains, inundation simulation conducted by using the satellite-based topography data and also using results from its applicability testing. The fourth section details a correction method for ALOS PRISM by using SRTM, followed by the fifth section, which describes the inundation simulation by using the corrected ALOS PRISM data. Finally, the sixth section summarizes the research.

2. COMPARISON OF SATELLITE-BASED TOPOGRAPHY DATA WITH LP

The three types of satellite-based topography data were compared with LP, a highly accurate topography data available for all river basins in Japan. Specifically, the elevation distribution and statistics of those satellite-based data were examined

2.1 Target area

The target area was the Nakanoshima District in the Kariyata River basin in Japan, where a major flood inundation occurred in July 2004. The area was selected because LP and other information (e.g., observed inundation areas) necessary to examine the performance of the satellite-based data are available.

2.2 Data

The three types of satellite-based topography data (ALOS PRISM, ASTER and SRTM) and LP were used as ground validation data in this research. Table 1 shows the spatial resolution and brief outline of each data.

Tab.1 The outline of LP and three satellite-based topography data

Data	Spatial Resolution	Brief outline
LP	2 m	Laser measurement by aircrafts
ALOS PRISM	10 m	Derived by stereo matching process of ALOS PRISM sensor data
ASTER	15 m	Derived by stereo matching process of ASTER sensor data
SRTM	90 m	Derived based on SAR sensor data on the space shuttle

2.3 Elevation distribution

Fig.1 shows the elevation distribution of each topography data over the target area of the flood inundation simulation described in the next section (East-West direction: about 4 km, North-South direction: about 12 km). The elevation distribution based on LP confirmed that the elevation in the target area decreases northward,

and the Kariyata River flows along the slope and merges into the Shinano River in the north-east section in the figure. The ASTER-based elevation shows rougher surface compared with the LP-based figure, and it is difficult to confirm the information obtained from the LP-based distribution. In addition, the ASTER-based distribution shows lower elevation than the LP-based distribution.. The SRTM-based elevation was roughest among the data with a mesh size of 90 m, and it is difficult to obtain detailed information on land surface such as the location of levees although it still shows the tendency of the elevation to decrease northward, which agrees with the information obtained from the LP-based data. On the other hand, ALOS PRISM does not show a clear northward decrease in elevation although land features such as a river or levees can be easily confirmed. At the same time, a swell-like characteristic is found around the center of the figure, which cannot be confirmed in the other types of topographic data.

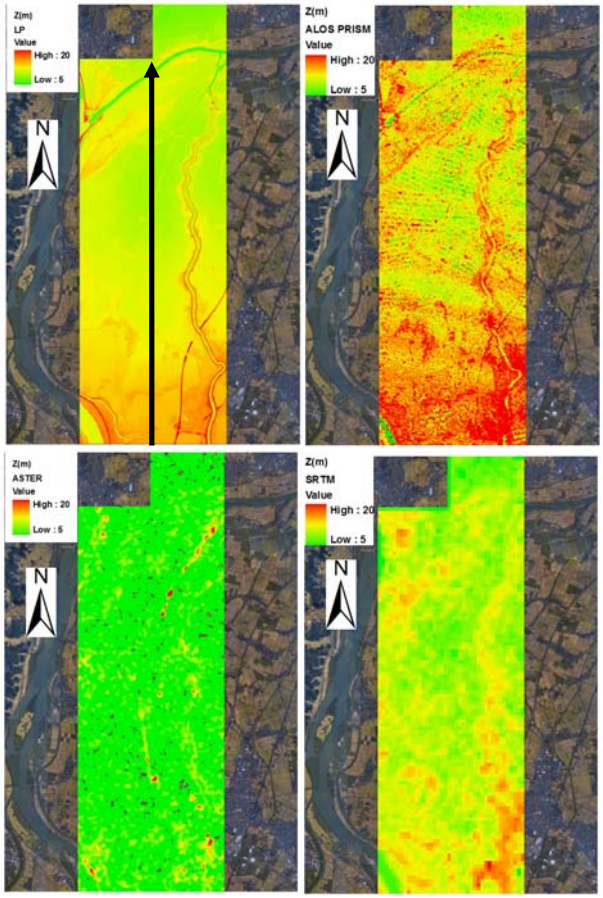

Fig.1 Distribution of elevation of four DSM data LP (upper left), ALOS PRISM (upper right), ASTER (lower left), SRTM (lower right)

2.4 Statistical accuracy evaluation

Statistical accuracy evaluation was conducted. The conditions for comparison are as follows.

1) Target area

The colored area in each figure of Fig.1 is the target area.

2) Ground truth data

LP was regarded as the ground truth data. with which ALOS PRISM, ASTER and SRTM were compared.

3) Comparison

In addition to the comparison in the original resolution of each data, the data were also compared in the same spatial resolutions by using two spatially averaged resolutions of 25 m and 100 m.

4) Method for comparison and spatial average

Because the original resolutions are different among the data, the number of samples of each data in the target area is also different. Knowing that statistical accuracy depends on the number of samples, that of each data type should be the same. For that reason, the following spatial averaging method was applied to make the number of samples of each data equal in the area.

In the comparison of the original resolutions, the target area was zoned into 100 m grids. The elevation of each data set was also plotted in original resolution. Comparison was then made between the satellite- and LP-based elevations whose grids share the same nearest 100 m grid.

Spatial average and comparison was conducted as follows. In the case of 25 m, for example, there were several grids of satellite-based topography data in the 25 m. The average elevation of those grids was simply derived by averaging those values . The same procedure is applied to LP, too. Then the averaged elevation which was closest to the 100 m grids used in the first step was compared with that of LP.

5) Statistical error index

Root mean square error (RMSE), mean error (M) and standard deviation (SD) were used as the statistical error indices in this study. The definition of each index is written as below.

a) Root Mean Square Error (RMSE)

$$RMSE = \sqrt{\{\sum_{i}^{N}(H_{Sat\_i} - H_{LP\_i})^2\} / N} \quad (1)$$

where N: the number of evaluation points

H_{Sat_i}: Elevation of ALOSPRISM, ASTER or SRTM,

H_{LP_i}: Elevation of LP data

b) Mean Error (M)

Mean error (M) was obtained by the equation below.

$$M = \{\sum_{i}^{N}(H_{Sat\_i} - H_{LP\_i})\} / N \quad (2)$$

c) Standard Deviation (SD)

Standard deviation (SD) was obtained by the equation below.

$$SD = \sqrt{[\sum_{i}^{N}\{(H_{Sat\_i} - H_{LP\_i}) - M\}^2] / N} \quad (3)$$

The comparison results of LP and ALOS PRISM, ASTER, SRTM are as presented below.

Tab. 2 Accuracy evaluation result of ALOS PRISM

	RMSE	M	SD
Original 10m	3.7	1.9	3.2
25m	3.3	1.8	2.8
100m	2.6	1.7	1.9

Tab. 3 Accuracy evaluation result of ASTER

	RMSE	M	SD
Original 15m	9.4	-8.5	3.9
25m	9.3	-8.5	3.8
100m	9.1	-8.5	3.2

Tab. 4 Accuracy evaluation result of SRTM

	RMSE	M	SD
Original 90m	2.6	-1.4	2.2
100m	2.3	-1.4	1.9

6) Comparison result

The comparison results of LP, ALOS PRISM, ASTER and SRTM are shown in Tab. 2, 3 and 4 for each resolution, respectively. The number of samples is 4,184 in this comparison.

a) ALOS PRISM

- The mean error was 1.7 m to 1.9 m and showed higher elevation compared with LP.
- The standard deviation became smaller with increase in mesh size. Averaging the mesh size made the error of each mesh averaged; as a result, the standard deviation became smaller.

b) ASTER

- The mean error was about -8.5 m and did not depend on mesh size. It was lower than LP as a whole.
- Both the RMSE and standard deviation did not become smaller when the mesh size became larger. ASTER did not show a decrease in mean error and standard deviation, unlike ALOS PRISM.

c) SRTM

- The mean error was -1.4 m. SRTM was lower than LP.
- Both the RMSE and standard deviation did not decrease when the mesh size became larger.

As a result, even though there was discrepancy between ALOS PRISM and SRTM in mean error, the RMSE and standard deviation showed almost the same value. ALOS PRISM overestimated the mean error at 1.7 m and SRTM underestimated it at 1.4 m. On the other hand, ASTER was inferior to ALOS PRISM and SRTM in all of the three terms.

2.5 Comparison in longitudinal section

In order to conduct visual examination on how the elevation of the satellite-based topography data approximates that of LP as the mesh size increases, a longitudinal section of LP, ALOS PRISM, ASTER and SRTM were compared in the original resolution and the averaged resolution of 100 m, while SRTM was compared only in 100 m since the original resolution was close to that value. The longitudinal section was examined in the south-north direction indicated in Fig. 1. The section was around 10,000 m long. The section started from the agricultural field in the south of the area, passed cities at the about 8,000 m point, and ended at the 10,000 m point, at which the Kariyata River meets with the Shinano River. Fig.2 shows the longitudinal elevation plotted based on each data in the south-north direction.

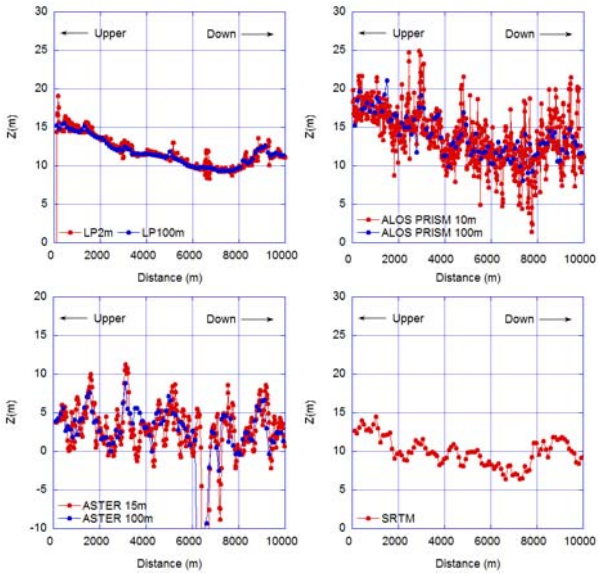

Fig.2 The longitudinal elevation of LP (upper left), ALOS PRISM (upper right), ASTER (lower left) and SRTM (lower right)

2.6 Summary of this section

The summary of this section is as follows.

- While it was difficult to obtain land features or structures such as levees from ASTER and SRTM due to their coarse spatial resolution, it was possible to recognize them from ALOS PRISM because of its fine resolution.
- By averaging the spatial resolution of ALOS PRISM, ASTER and SRTM to 100 m, the mean error of those data were estimated at +1.4 m, -8.5 m and -1.4 m, respectively. While ALOS PRISM and SRTM showed almost the same value on RMSE and standard deviation, ASTER was inferior to them.
- ALOS PRISM and SRTM showed agreement with LP in the overall gradient of the longitudinal section, but were not so accurate as LP.

3. FLOOD INUNDATION SIMULATION WITH THE SATELLITE-BASED TOPOGRAPHY DATA IN THE KARIYATA RIVER BASIN

3.1 Overview and flow of the study in this section

Flood inundation simulation was conducted over the target area by using ALOS PRISM, ASTER and SRTM to examine the applicability of the satellite-based

topography data to inundation simulation in the following steps.

1) Inundation simulation was conducted by using LP as a topography data. The July 2004 flood in the Kariyata River Basin was studied as the case study in this section.
2) The inundation simulation results from 1) were compared with the observed inundation area[4]. If the simulation results did not agree very well with the observation, simulation was repeated with different conditions such as different roughness coefficients and other parameters until the results agree with the observation. Because it was assumed that inundation simulation by using satellite-based topography data cannot reproduce the actual inundation depth, the inundation area observed in the July 2004 flood event at the Kariyata River basin was selected as the target of the inundation simulation[4].
3) When the validity of the inundation simulation was confirmed, inundation simulation was conducted based on the satellite-based data (hanged to ALOS PRISM, ASTER and SRTM) and their performance was studied respectively.

3.2 Inundation simulation of the July 2004 flood by using LP

1) Inundation model

In this study, a 2D flood inundation simulation model was used[5].

2) Mesh size

The mesh size was set at 100 m because the target area was about 50 km^2. The area is mostly used as farmland, and the slope is fairly mild.

3) Flood inundation discharge from the levee breach point

Runoff calculation was conducted to estimate river discharge at the levee breach point under two conditions: "without levee breach" and "with levee breach"[6]. In this study, the discharge difference in simulation results between these two conditions was regarded as the levee breach discharge flowing into the inundation area and used as the input for inundation simulation. Fig.3 shows the hydrograph after the levee breach.

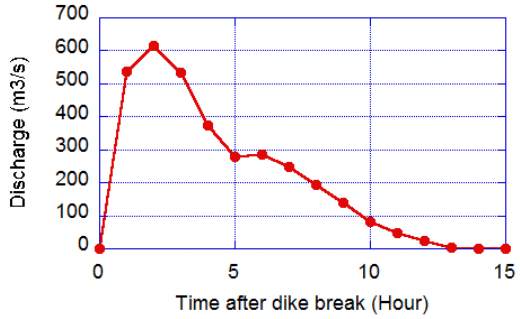

Fig.3 Hydrograph of levee breach

4) Structures

Structures such as channels in the target area were not considered in this study because the aim of the study was to simulate an approximate area of flood inundation, not to simulate accurate inundation depth.

5) Results of inundation simulation

Flood inundation simulation was conducted at intervals of 10 seconds under the two conditions described above. Fig.4 shows the simulation results and the observed inundation areas[4]. The simulation results showed an acceptable agreement with the observed inundation area. Then, only the topography data set, i.e., LP, was changed alternatively to one of the three satellite-based topography data (ALOS PRISM, ASTER and SRTM) with the other conditions left unchanged.

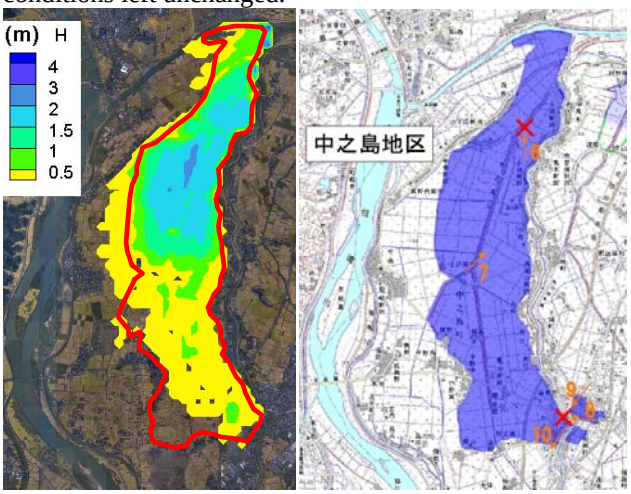

Fig.4 The result of flood inundation simulation (Left: simulation, Right: observed inundation area[4])

3.3 Flood inundation simulation by using ALOS PRISM, ASTER and SRTM

Fig.5 shows the results of flood inundation simulation by using LP, ALOS PRISM, ASTER and SRTM. They each show the inundation 9 hours after the levee breach. The head of the flood waters has reached the confluence of the Kariyata and Shinano Rivers by then in the LP-based simulation and become stable. The ALOS PRISM-based simulation appears differently in that the inundation flow stops at the swelling part described in section 2.3. The ASTER-based result looks similar to that of ALOS PRISM. The simulation does not reproduce the downward flow of the inundation water very well probably because ASTER is rough in elevation. The SRTM-based simulation reproduces the actual inundation area better than the other two. However, the flood waters based on SRTM has not reached the confluence of the two rivers when it has in the LP simulation.

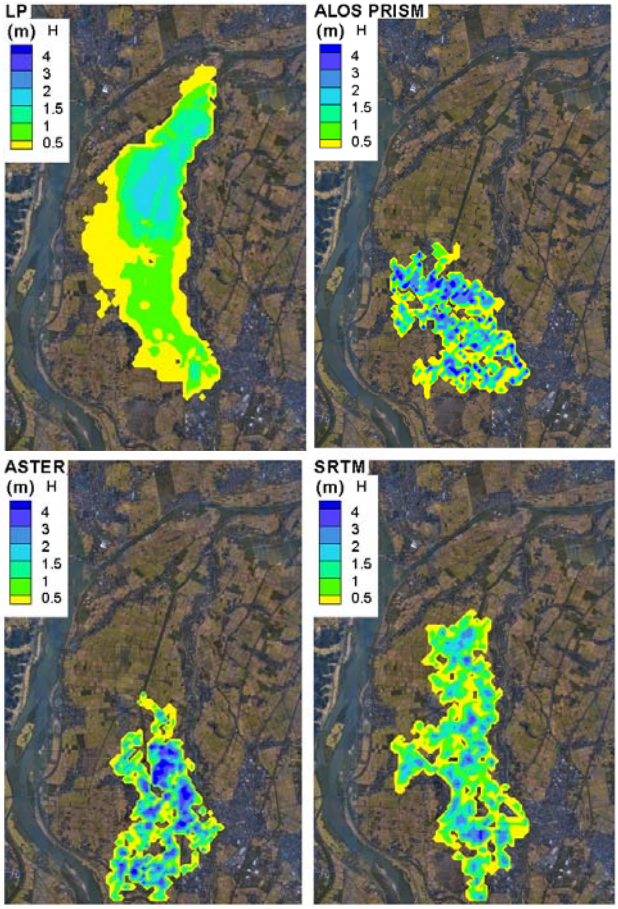

Fig.5 The result of flood inundation simulation 9 hours after levee breach (distribution of inundation depth) (Upper left: LP, Upper right: ALOS PRISM, Lower left: ASTER, Lower right: SRTM)

3.4 Discussion and summary of this section

As a result of the flood inundation simulation based on three satellite-based topography data (ALOS PRISM, ASTER and SRTM), it was confirmed that any of the simulations did not reproduce the actual inundation area. This is due to the accuracy level of the satellite-based topography data. The statistical values such as mean error, standard deviation and RMSE of ALOS PRISM could have been reduced by averaging the mesh size from the original 10 m to 100 m. However, even though ALOS PRISM and SRTM could express the overall gradient of the actual land surface in the averaged 100 m mesh size, the roughness could not be eliminated completely and there were still discrepancies from the elevation of LP. Because the roughnesses of ALOS PRISM and SRTM in elevation is larger than that of LP, the moving speed of the flood waters was slower than the actual speed.

In order to reproduce the actual inundation area by using the satellite-based topography data, the mesh size has to be at least larger than 100 m so that the elevation of ALOS PRISM and SRTM will approximate that of LP. Because the area of flood inundation examined in this study was only about several tens km^2, however, inundation simulation using a mesh size of more than 100 m may not be appropriate. Therefore, satellite-based topography data should be applied to flood inundation whose area is much larger than that in the target area of this study by averaging the mesh size into a much larger size than 100 m. In order to utilize the satellite-based topography data for flood inundation as large as that in this study, not only spatial averaging but also a statistical correction method is required.

4. DETAILED ASSESSMENT OF THE ACCURACY OF THE DSM DERIVED FROM ALOS PRISM

In the previous section, the applicability of satellite-based topography data to the flood inundation was examined and concluded that a statistical correction method is necessary to obtain acceptable flood inundation simulation results. In this section, a detailed assessment of the accuracy of satellite-based topography data was conducted to get to an idea how to correct the satellite-based topography data statistically. The effect of land use on the accuracy was especially examined. Only the DSM derived from ALOS PRISM was studied in this section because the spatial resolution is the finest among the three satellite-based topography data.

4.1 The experimental area and the data

1) The experimental area

The experimental area in this section is the surrounding area of the Watarase Retarding Basin because there are several land use such as urban areas and agricultural fields. In addition to that LP data is available in the area.

2) ALOS PRISM data

In this section, 4 DSMs of ALOS PRISM were used to conduct the detailed statistical error analysis. According to the survey on the availability of ALOS PRISM data in this area, it was found that 4 scenes which were observed in different date were available. Tab.5 shows the 4 scenes of ALOS PRISM data which were used in this section. The yellow box shown in Fig.6 shows the area in which 4 scenes are overlapped and the area in light blue area was the area in which a statistical analysis was conducted. Because No.4 scene was covered with cloud largely, it was used only for the agricultural fields described next.

Tab.5 ALOS PRISM scenes used in this section

No.	ID	Date of observation	Mode*)	Name
1	ALPSMN159142870	2009/01/19	OB1	PSM-DSM1
2	ALPSMN208592870	2009/12/24	OB1	PSM-DSM2
3	ALPSMW248852870	2010/09/26	OB2	PSM-DSM3
4	ALPSMW199402870	2009/10/22	OB2	PSM-DSM4

*) OB1: DSM derived by triplet stereo matching. OB2: DSM derived by doublet stereo matching.

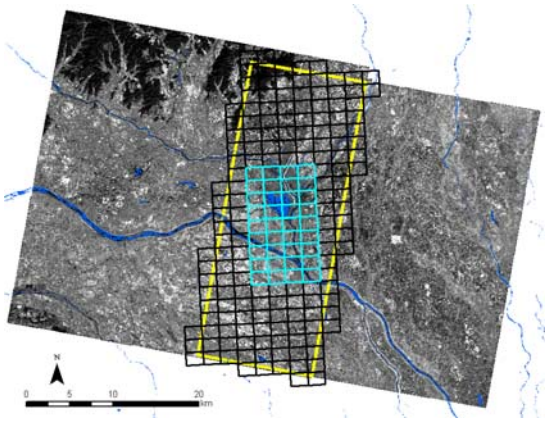

Fig.6 The experimental area (All 4 scenes were available in the area surrounded by yellow box. The area surrounded by light blue box shows the experimental area in this section.)

3) The study area

The area which was surrounded by light blue box in Fig.6 contains several land use. In this section, three specific areas were selected by referring the land use in the experimental area. The three areas mainly include agricultural field, urban area and large river dykes respectively (Fig.7). Each ALOS PRISM DSM was compared with LP data and its accuracy was examined respectively.

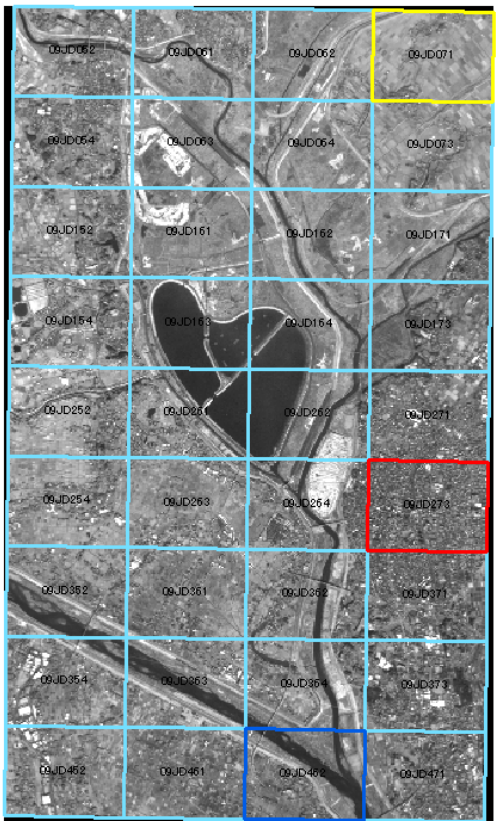

Fig.7 Three selected areas (yellow: agricultural field, red: urban area, blue: area in which the large dykes are included.)

4.2 Comparison results

1) Agricultural field

Tab.6 shows the error statistics of each scene in the agricultural field. Concerning standard deviation (hereinafter SD) and root mean square error (hereinafter RMSE), only PSM-DSM3 showed different characteristics compared with other scenes. The OB1 products, PSM-DSM1 and PSM-DSM2 showed almost same statistical characteristics. However, as shown Fig.8 and Fig.9, the error distribution did not look similar. There are not only agricultural fields but also some houses in this area. The error distribution looks similar between the two in the area in which there are houses. However, in other agricultural fields, the error distribution was different between the two. This shows the possibility that ALOS PRISM has the randomness in agricultural fields. Fig. 10 shows the altitude of the line shown in red line in Fig. 11. According to Fig.11, the error characteristics of each scene are completely different between them. There were the sections in which a scene showed larger than LP and other showed lower.

Tab.6 Error statistics in the agricultural field

Name	bias (m)	SD (m)	RMSE (m)
PSM-DSM1	+0.73	3.56	3.60
PSM-DSM2	-0.41	3.39	3.45
PSM-DSM3	+2.93	3.09	4.13
PSM-DSM4	+0.54	3.87	3.89

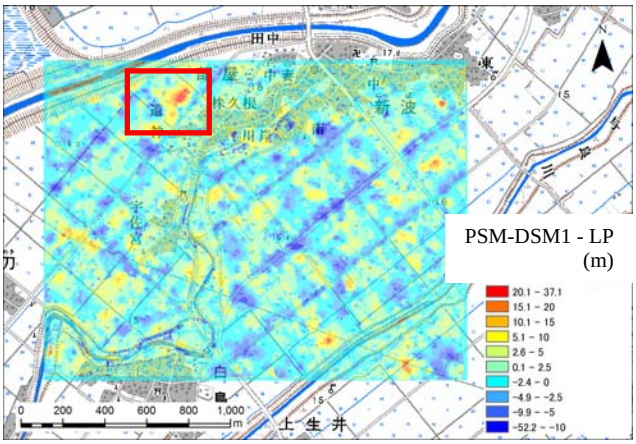

Fig.8 Difference between LP and PSM-DSM1 (agricultural area)

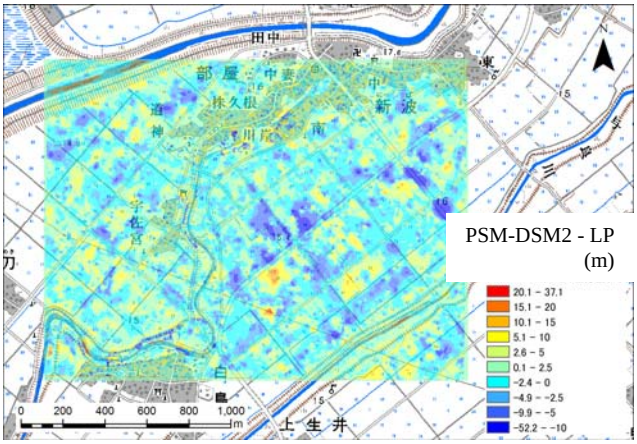

Fig.9 Difference between LP and PSM-DSM2 (agricultural area)

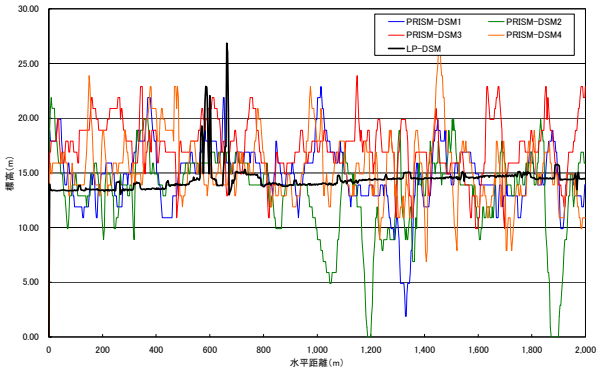

Fig.10 Cross sectional elevation of the agricultural area

Fig.11 A stereo image of yellow-boxed agricultural area of Fig.7 (Scene No.1)

2) Urban area

Tab.7 showed SD and RMSE of each ALOS PRISM in the urban area. As a result, SD and RMSE of PSM-DSM3 were larger than that of other two scenes. This is probably due to the and there were not clear differences between PSM-DSM1 and PSM-DSM2. Fig.12 and Fig.13 showed the distribution of differences between PSM-DSM1, 2 and LP. According to these figures, the error distribution of PSM-DSM1 and PSM-DSM2 showed similarity. In the agricultural fields, as mentioned before, the error characteristics of PSM-DSM1 and PSM-DSM2 were almost similar statistically but the error distribution was different spatially. However, in the urban area, both statistically and spatially, the error characteristics were similar between PSM-DSM1 and PSM-DSM2. Fig.14 showed the altitude along the red line shown in Fig.15. In the agricultural field, there were some sections in which a scene showed larger than LP but other scenes lower. On the contrary, in this urban area, it can be confirmed that each scene had error to some extent but all three scenes showed same tendency.

Tab.7 Error statistics in the urban area

Name	Date of observation	Bias (m)	SD (m)	RMSE (m)
PSM-DSM1	2009/01/19	+ 2.26	4.56	4.97
PSM-DSM2	2009/12/24	+ 0.74	4.59	4.62
PSM-DSM3	2010/09/26	+ 3.02	4.92	5.64

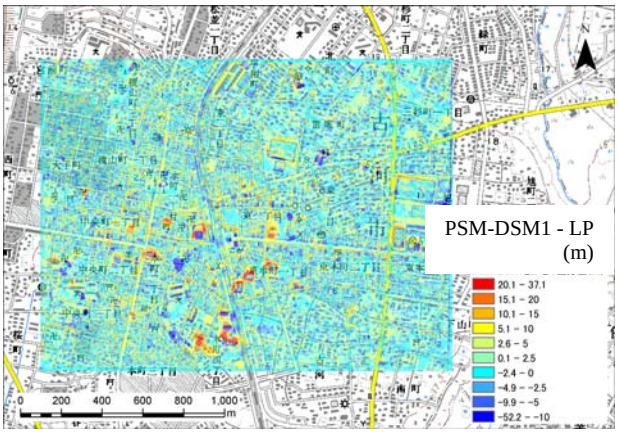

Fig.12 Difference between LP and PSM-DSM1

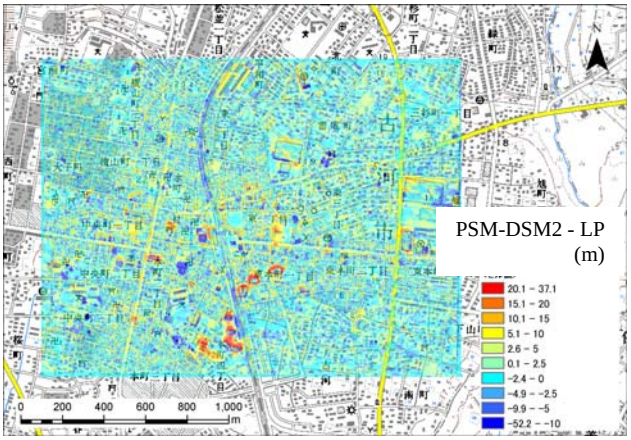

Fig.13 Difference between LP and PSM-DSM2

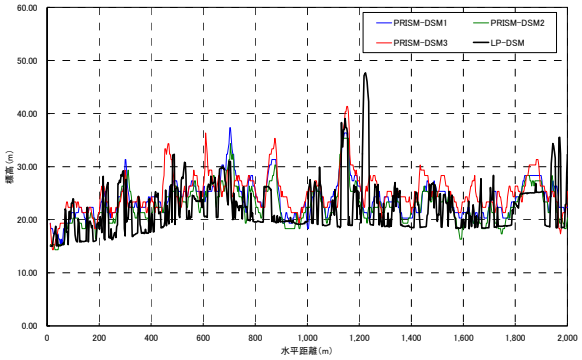

Fig.14 Cross section along the red line in Fig.15

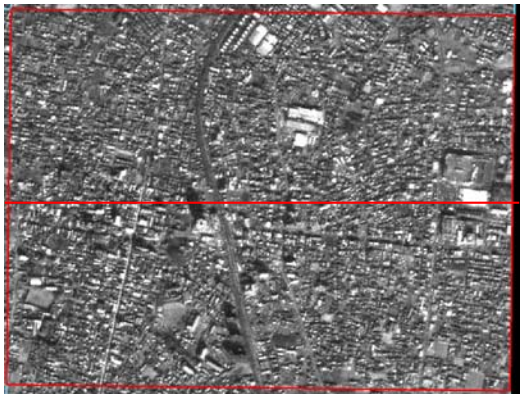

Fig.15 A stereo image of the red-boxed urban area of Fig.7 (Scene No.1)

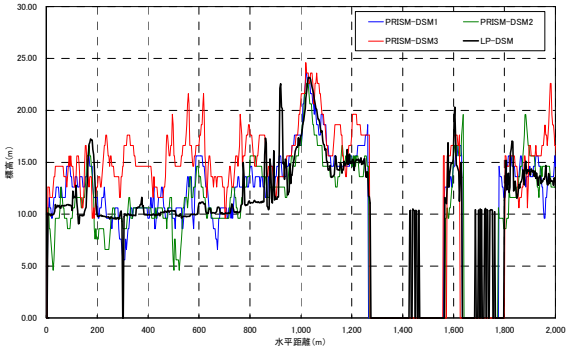

Fig.16 Cross section in the red line of Fig.17

Fig.17 A stereo image of the blue-boxed area with dykes (Scene No.1)

3) The area in which the large dyke is included

In the area in which the large dykes were included, there are not only the dykes but also agricultural fields. Fig.16 showed the altitude along the red line shown in Fig.17. The main land use in the section from 0 to 800 m was agricultural fields. The error characteristics of each scene in this section were almost same with that in 4.2 1) and each error looked random. On the other hand, there was the large dyke in the section from 900 m to 1,100 m in Fig.16. All of three scenes showed relatively same characteristics and the shape of the levee were expressed by all of the scenes respectively.

4.3 Discussion

According to the experiments in the three areas, it was suggested that each scene of ALOS PRISM showed same tendency in urban areas and for large dykes. For urban areas and dykes, surface condition usually does not change very much and the existence of the sharp land features such as buildings or dykes make the accuracy of the stereo matching higher. On the contrary, surface condition in agricultural fields change seasonally. In addition to that, the stereo matching in agricultural fields is considered as more difficult than that in urban area and for large dykes because the stereo matching on crops or grasses/plants are usually considered to be difficult. Fig.18 is the focus of the red box drawn in Fig.8 and the large error can be confirmed (the red circled area). Fig.19 is the stereo image of the scene No.1 for the same area with Fig.18. It can be seen that the image was blurred in the red circle in Fig.19 corresponding to the circled area in Fig.18, in which the large error was confirmed. From these figures, it is suggested that the low accuracy on stereo matching in agricultural fields is the cause of the result with low accuracy of ALOS PRISM DSM in this study.

Our main purpose to use satellite-based topography data is to conduct flood inundation simulation in developing countries in which precise topography data such as LP are not available. Major land use in developing countries is thought to be agricultural fields and flood disaster occurs in those areas accordingly. However, as a result of this section, the ALOS PRISM DSMs showed relatively low accuracy in such agricultural fields. The error which is considered to be due to low stereo matching accuracy should be eliminated in order to use ALOS PRISM DSMs for flood inundation simulations. A strategy to correct ALOS PRISM DSMs would be eliminating elevation values in which stereo matching accuracy is low at first and replacing the eliminated values with those in which stereo matching accuracy are high. Another strategy for the correction in agricultural fields would be just simply averaging many temporal scenes for the specific target area because the error seems random in agricultural fields. To confirm them is the future subject.

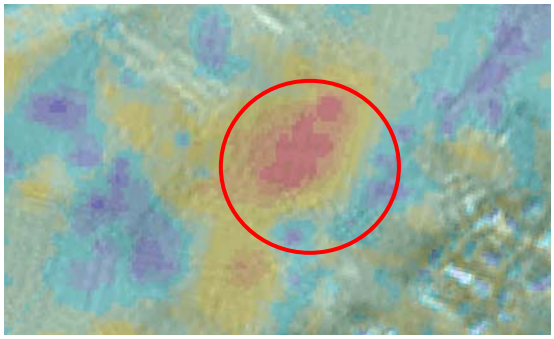

Fig.18 Focus of the area in which large error is confirmed in Fig.8

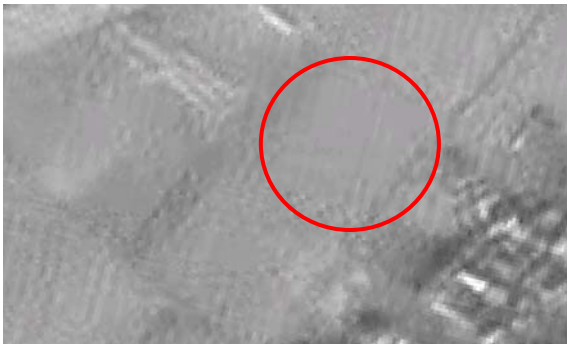

Fig.19 Stereo image of the focused area above (Scene No.1)

5. CONCLUSION

The conclusions in this report are summarized as below.

1. Basic characteristics of satellite-based topography data are as follows:

- While it was difficult to obtain land features or structures such as levees from ASTER and SRTM due to their coarse spatial resolution, it was possible to recognize them from ALOS PRISM because of its fine resolution.
- By averaging the spatial resolution of ALOS PRISM, ASTER and SRTM to 100 m, the mean error of those data were estimated at +1.4 m, -8.5 m and -1.4 m, respectively. While ALOS PRISM and SRTM showed almost the same value on RMSE and standard deviation, ASTER was inferior to them.
- ALOS PRISM and SRTM showed good agreement with LP in the overall gradient of the longitudinal section, but were rougher in elevation than LP.

2. Applicability of satellite-based DSM to flood inundation simulation is as follows:

- As a result of the flood inundation simulation (the flood inundation event in the Kariyata River Basin in 2004) based on three satellite-based topography data (ALOS PRISM, ASTER and SRTM), it was confirmed that any of the simulations did not reproduce the actual inundation area.
- Satellite-based topography data usually have large and many roughness which cannot be confirmed in LP. This makes the accuracy of the flood inundation simulation by satellite-based topography data low.
- In order to reproduce the actual inundation area by using the satellite-based topography data, the mesh size has to be at least larger than 100 m so that the elevation of ALOS PRISM and SRTM will approximate that of LP.
- In order to utilize the satellite-based topography data for the flood inundation in the Kariyata River Basin in 2004, not only spatial averaging but also a statistical correction method are required.

3. Detailed assessment of the accuracy of the DSM derived from ALOS PRISM

- It was confirmed that each scene of ALOS PRISM showed almost same error characteristics for urban areas and large dykes. On the other hand error showed randomness for agricultural fields in which stereo matching is more difficult compared with that in urban area and for large dykes.
- Random error of DSMs of ALOS PRISM confirmed in agricultural fields should be eliminated by referring information on the rate of stereo matching. A strategy to correct ALOS PRISM DSMs would be eliminating elevation values in which stereo matching accuracy is low at first and replacing the eliminated values with those in which stereo matching accuracy are high. Another strategy for correction in agricultural fields would be just simply averaging many scenes for the target area because the error seens random in agricultural fields.

6. ACKNOLEDGEMENT

The authors express sincere thanks to ALOS-PRISM Science Team of JAXA-EORC, in particular, Dr. Takeo TADONO, for their special contribution to the preparation of ALOS-PRISM DSMs.

7.REFERENCES

[1] Sekine M., J. Nakamura and Y. Nakamura: Numerical analysis of inundation caused by a heavy rainfall and an overflow from the Shakujii-Gawa river in 2005, Annual Journal of Hydraulic Engineering, pp.865-870, Feb. 2008 (in Japanese)

[2] Tsubaki R., I. Fujita and T. Okabe: Unstructured grid generation using LIDAR measurement for inundation analysis, JSCE Journal of Hydraulic, Coastal and Environmental Engineering, Vol.62, No.1, pp.41-52, 2006 (in Japanese)

[3] Iwata K., Y. Shimizu: 2D calculation study of flood damage in urban area at Apia, Samoa Island, Annual Journal of Hydraulic Engineering, pp.835-840, Feb. 2008 (in Japanese)

[4] Geospatial Information Authority of Japan (GSI): Inundated area by the heavy rainfall in Niigata and Fukushima (Sanjo, Mitsuke and Nakanoshima), http://www.gsi.go.jp/BOUSAI/SAIGAI/16niigata/higai-zyoukyou-niigata_suigai.html (in Japanese)

[5] Japan Society of Civil Engineers: Hydraulics Formulae: Hydraulics Worked Examples with CD-ROM, March 2002 (in Japanese)

[6] Committee on survey of the flood disaster by the heavy rainfall in Niigata July 13th (in Japanese)